The Astrophysical Journal Letters, 869:L23 (5pp), 2018 December 20 https://doi.org/10.3847/2041-8213/aaf4b8

The Correlation between Isotropic Energy and Duration of Gamma-Ray Bursts

Z. L. Tu[1] and F. Y. Wang[1,2]
[1] School of Astronomy and Space Science, Nanjing University, Nanjing 210093, People's Republic of China; fayinwang@nju.edu.cn
[2] Key Laboratory of Modern Astronomy and Astrophysics (Nanjing University), Ministry of Education, Nanjing 210093, People's Republic of China
Received 2018 November 7; revised 2018 November 28; accepted 2018 November 29; published 2018 December 13

Abstract

In this Letter, we study the correlation between isotropic energy and duration of gamma-ray bursts (GRBs) for the first time. The correlation is found to be $T_{\rm duration} \propto E_{\rm iso}^{0.34\pm0.03}$ from the *Swift* GRB sample. After comparing with solar flares from *RHESSI* and stellar superflares from the *Kepler* satellite, we find that the correlation of GRBs shows a similar exponent with those of solar flares and stellar superflares. Inspired by the physical mechanism of solar flares and stellar superflares, magnetic reconnection, Inspired by treating magnetic reconnection as the physical mechanism of solar flares, we interpret the correlation using magnetic reconnection theory. This similarity suggests that magnetic reconnection may dominate the energy-releasing process of GRBs.

Key words: gamma-ray burst: general – stars: flare

1. Introduction

Gamma-ray bursts (GRBs) are explosive phenomena occurring at cosmological distance (Kumar & Zhang 2015; Wang et al. 2015; Zhang et al. 2016), and they play a vital role in multi-messenger astronomy (Willingale & Mészáros 2017, etc.). As the central engine is still mysterious, numerous theories have been proposed to explain the burst prompt emission mechanism or central engine (Beloborodov & Mészáros 2017; Dai et al. 2017; Nagataki 2018), including the internal shock model (Rees & Meszaros 1994; Daigne et al. 2011), the dissipative photosphere model (Spruit et al. 2001; Rees & Mészáros 2005), the electromagnetic model (Lyutikov & Blandford 2003; Lyutikov 2006) and the internal-collision-induced magnetic reconnection and turbulence model (Zhang & Yan 2011). Although they have successfully interpreted some remarkable GRBs, there are still some open questions.

Because there are many models for interpreting the physical mechanism of GRBs, it is essential to statistically analyze the basic properties of GRBs. Hou et al. (2013) discussed whether or not there is a correlation between isotropic energy and duration of GRBs. Some empirical correlations have been found (Wang et al. 2015; Dainotti & Del Vecchio 2017; Dainotti & Amati 2018; Dainotti et al. 2018), e.g., the isotropic energy and spectral peak energy correlation $E_{\rm iso}$–E_p (Amati et al. 2002; Wang et al. 2016), the correlation between $E_{\rm iso}$, spectral peak energy E_p and the rest-frame break time t_b (Liang & Zhang 2005), X-ray luminosity L_X and the rest-frame time of plateau phase T_a^* (Dainotti et al. 2015), lag–luminosity correlation $\tau_{\rm lag}$–$L_{\rm iso}$ (Norris et al. 2000), and the fundamental plane of GRBs (Dainotti et al. 2016, 2017a). However, the correlation between duration and isotropic energy has yet to be studied.

Stellar superflares are violent energy-releasing events occurring on the stellar surface. Maehara et al. (2012) statistically studied the superflares from solar-type stars, by virtue of continuously long periods of observation by *Kepler*. Both long- and short-cadence data from *Kepler* have been collected to study superflares compared with solar flares (Shibayama et al. 2013; Maehara et al. 2015, etc.). To be specific, Maehara et al. (2015) fitted the correlation between the duration and energy of stellar superflares as $\tau_{\rm flare} \propto E_{\rm flare}^{0.39\pm0.03}$, which is comparable to the statistical analysis of solar flares.

In this Letter, the correlation between duration and isotropic energy of GRBs is fitted. While filling a vacancy of statistical correlation studies of GRBs, we explore potential resemblances between stellar flares and GRBs. In order to make comparison, solar flares from *RHESSI* and superflares of solar-type stars from *Kepler* are gathered here. Linear regression has been performed with different kinds of data. In order to test if our fitting results are strongly credible, statistical methods *t*-test and *F*-test are utilized. Throughout this Letter, we adopt cosmological parameters as $H_0 = 67.7\,{\rm km\,s^{-1}\,Mpc^{-1}}$, $\Omega_m = 0.31$, $\Omega_\Lambda = 0.69$ (Planck Collaboration et al. 2016).

This Letter is structured as follows. Samples of GRBs, solar flares from *RHESSI*, and superflares of solar-type stars from *Kepler* are presented in Section 2. The results of linear regression in log–log fields are given in Section 3. In Section 4, we give a reasonable explanation of the correlation basing on magnetic reconnection. Conclusions and discussion are given in Section 5.

2. Data Samples

This section will specifically introduce the filter conditions of data selection. Methods of calculation for different data sets will also be presented.

2.1. Gamma-Ray Bursts

Swift has observed GRBs since 2004, and over 1000 GRBs have been detected. In this Letter, we select those GRBs with redshift measurements during 2005 January to 2018 November. In order to avoid importing system errors from different GRB surveys, we only use GRBs from the website of the *Swift* data table.[3] In addition to redshift, duration time T_{90} and fluence of prompt emission $S_{\rm GRB}$ with 90% error can also be obtained from the website. Those GRBs showing an absence of duration time or error of fluence are excluded from the database. We then use the redshift measurements for GRBs from Jochen Greiner's website.[4] There are total of 386 GRBs for further study.

[3] https://swift.gsfc.nasa.gov/archive/grb_table/
[4] http://www.mpe.mpg.de/~jcg/grbgen.html

Table 1
Fitting Results

Data Set Satellite	GRBs *Swift*	Solar Flares *RHESSI*	Stellar Superflares *Kepler*
k	0.34 ± 0.032	0.33 ± 0.00093	0.39 ± 0.025
b	-16.36 ± 1.64	0.95 ± 0.0045	-12.14 ± 0.86
σ_v	0.66 ± 0.024	0.24 ± 0.00051	0.25 ± 0.013
r	0.47	0.72	0.75
t	10.32	350.82	15.48
$t_{5\%/2}$	1.97	1.96	1.97
F	106.58	123076.52	239.52
$F_{5\%}$	3.87	3.84	3.89

Note. k and b represent slope and intercept of linear regression, respectively. σ_v is extra variability. r gives the correlation coefficient. $t_{5\%/2}$ and $F_{5\%}$ are upper limits of the t- and F-distribution at 5% possibility. The fitting results of t and F are greater than $t_{5\%/2}$ and $F_{5\%}$, respectively.

Because GRBs occur at cosmological distances, the time should be transferred to the rest frame. The duration can be written as

$$T_{\rm GRB,duration} = \frac{T_{90}}{1+z}. \tag{1}$$

The isotropic energy is

$$E_{\rm GRB,iso} = \frac{4\pi D_{\rm L}^2 S_{\rm GRB}}{1+z}, \tag{2}$$

where $D_{\rm L}$ is luminosity distance which relates to cosmological parameters. $S_{\rm GRB}$ represents fluence.

2.2. Solar Flares

Solar flares have been studied since their first observation in 1859 (Carrington 1859). The *RHESSI* spacecraft has been manipulated successfully over 16 years. More than 120,000 solar flares have been observed from 2002 to 2018, and they are listed online.[5] The bolometric energy of a flare can be calculated by summing the energy of each detected photon. To avoid obtaining the energy spectrum of each flare, we use the total counts to represent the total energy of solar flares. The energy is proportional to the total counts, which can be expressed as

$$E_{\rm flare} \propto C_{\rm total}. \tag{3}$$

Because instrumental sensitivity decreases below the ~5 keV band, the total counts are taken from 6 to 12 keV energy range (Christe et al. 2008). The online list includes some flags marking non-solar events (NSs) and possible solar flares (PSs). After eliminating flares marked as NS or PS, 114,728 solar flares are used in this Letter. Their total counts $C_{\rm total}$ and duration time of solar flares $T_{\rm solar,duration}$ are directly obtained from the flare list.

2.3. Superflares of Solar-type Stars

In this Letter, we also consider the superflares of solar-type stars. Maehara et al. (2015) selected 23 solar-type stars with 187 white-light superflares from 18 quarters of *Kepler* short-cadence data. We obtain the properties of these superflares, including energy of flares $E_{\rm superflares}$ and duration $T_{\rm superflares}$ (Maehara et al. 2015). To be specific, the duration $T_{\rm superflares}$ is derived from the e-folding decay time.

[5] https://hesperia.gsfc.nasa.gov/hessidata/dbase/hessi_flare_list.txt

3. Methods and Results

3.1. Linear Regression

We use the duration and energy from different data sets to constrain the power-law correlation

$$T = 10^b \times E^k, \tag{4}$$

where energy E is substituted as $C_{\rm total}$ for solar flares, and T represents duration of different data. We take $y = \log_{10} T$ and $x = \log_{10} E$ in log–log fields. Then this correlation can be derived as

$$y = kx + b, \tag{5}$$

where k and b are fitted from linear regression in this Letter.

We use the maximum likelihood method to perform linear regression. The general likelihood can be written as (D'Agostini 2005)

$$\mathcal{L} \propto \prod_i \frac{1}{\sqrt{\sigma_v^2 + \sigma_{y_i}^2 + k^2\sigma_{x_i}^2}} \times \exp\left[-\frac{(y_i - kx_i - b)}{2(\sigma_v^2 + \sigma_{y_i}^2 + k^2\sigma_{x_i}^2)}\right], \tag{6}$$

where σ_v is extra variability. σ_{x_i} and σ_{y_i} are variants taken from observations. We take $\sigma_{x_i} = 0$ and $\sigma_{y_i} = 0$ for solar flares and superflares of solar-type stars, due to the errors that are not included in database.

3.2. Testing Significance of Regression

In order to test the significance of regression, t-tests and F-tests methods are imported in this Letter. In short, these methods are used to quantitatively test whether or not the slope of linear regression can reject a null slope hypothesis, and describe the compactness between the slope of correlation and data. The $t_{\rm value}$ can be written as (Montgomery et al. 2012)

$$t_{\rm value} = \frac{(k - k_0)\sqrt{(n-2)\sum_{i=1}^n (x_i - \bar{x})^2}}{\sqrt{\sum_{i=1}^n (y_i - kx_i - b)^2}}, \tag{7}$$

where k and b are the results of regression. x_i and y_i are properties from observational data. n is the number of data points. $\bar{x}$ gives the mean value of x_i. The null hypothesis means $k_0 = 0$. If

$$|t_{\rm value}| > t_{\alpha/2,n-2}, \tag{8}$$

then the null hypothesis is rejected at the upper percentage point, where $t_{\alpha/2,n-2}$ represents the rejection regions of t distribution. Here we take $\alpha = 5\%$.

An F-test is also imported in this Letter as a replenishment of the t-test. The $F_{\rm value}$ can be written as (Montgomery et al. 2012)

$$F_{\rm value} = \frac{(n-2)\sum_{i=1}^n (kx_i + b - \bar{y})^2}{\sum_{i=1}^n (y_i - kx_i - b)^2}, \tag{9}$$

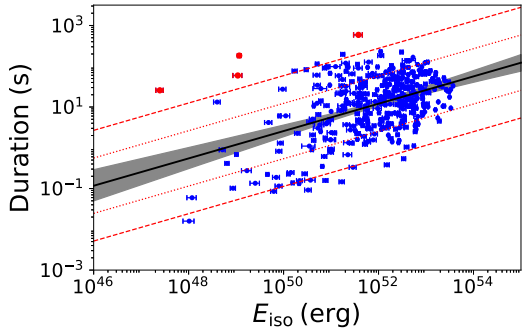

Figure 1. Linear fitting of GRBs. The black solid line represents the fitting result in log–log field. The red dotted and dashed lines represent $1\sigma_v$ and $2\sigma_v$ regions of extra variabilities, and the gray area stands for a 95% confidence interval of fitting uncertainties. The four red points located far outside of the $2\sigma_v$ region are GRB 111005A, GRB 080517, GRB 101225A, and GRB 171205A.

where $\bar{y}$ gives mean of y_i. Referring to t-test, we take the $F_{\alpha,1,n-2}$ of the F-distribution as rejection regions. If

$$F_{\rm value} > F_{\alpha,1,n-2}, \tag{10}$$

then the null hypothesis is rejected. $\alpha = 5\%$ is also applied to the F-test.

3.3. Results

The results of regression and statistical variances of different data sets are presented in Table 1. For each kind of data, the power-law relation between duration and releasing energy are fitted.

After applying linear regression in log–log fields, we get the relation of GRBs as

$$T_{\rm GRB,duration} \propto {E_{\rm GRB,iso}}^{0.34\pm0.032}. \tag{11}$$

Figure 1 gives the result of linear regression. The correlation coefficient is $r = 0.47$, and $\sigma_v = 0.66 \pm 0.024$. The result of the t-test is $|t_{\rm value}| \approx 10.32$, which is larger than the rejection region at $t_{2.5\%,308-2} = 1.97$. The F-test gives $F_{\rm value} \approx 106.58$, which is greater than $F_{5\%,1,308-2} = 3.87$. These results strengthen our belief that the duration is correlated with isotropic energy. In Figure 1, four red points are located outside of the $2\sigma_v$ area, which are GRB 111005A, GRB 080517, GRB 101225A, and GRB 171205A. These are extraordinary GRBs, showing low luminosity or ultra-long duration (Levan et al. 2014; Stanway et al. 2015; Dado & Dar 2017; MichałowskI et al. 2018).

It should be noted that the selection biases may be important, although this is outside the scope of this Letter. Kocevski & Petrosian (2013) used simulated GRBs to propose that the duration of GRBs may not be dilated by cosmological expansion but decreased by detectors, due to the diminishing signal-to-noise ratio. At high redshift, only the brightest GRBs can be detected. Some works concluded that the duration of the GRB is mainly affected by cosmological dilation (e.g., Zhang et al. 2013; Littlejohns & Butler 2014). Recently, Lloyd-Ronning et al. (2018) found an anti-correlation between source frame durations and the redshifts of radio-loud GRBs. Consequently, the Efron & Petrosian (1992) method, which has been broadly used (e.g., Lloyd & Petrosian 1999; Dainotti et al. 2013, 2015, 2017b; Yu et al. 2016; Zhang & Wang 2018), needs to be applied in order to reveal the nature of $T_{\rm GRB,duration}$–$E_{\rm GRB,iso}$ correlation.

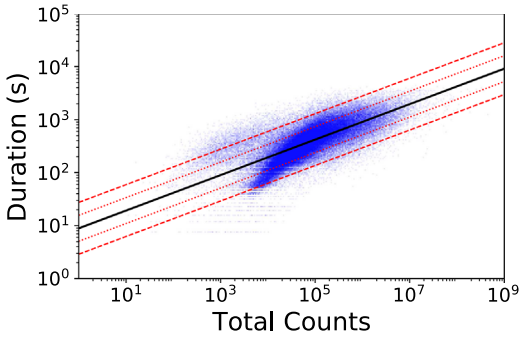

Figure 2. Linear fitting of solar flares. The black solid line represents the result of fitting in log–log field. The red dotted and dashed lines represent $1\sigma_v$ and $2\sigma_v$ regions of extra variabilities, and the gray area stands for a 95% confidence interval of fitting uncertainties. Because the error of this fitting result is tiny, the black solid line and the gray area are overlapped.

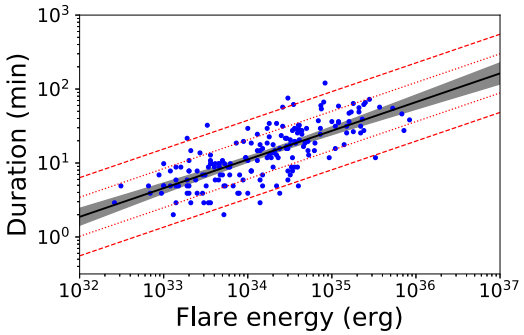

Figure 3. Linear fitting of stellar superflares. The black solid line represents the best fitting in log–log field. Red dotted and dashed lines represent $1\sigma_v$ and $2\sigma_v$ regions of extra variabilities, and the gray area stands for a 95% confidence interval of fitting uncertainties.

The linear regression of solar flares gives

$$T_{\rm solar,duration} \propto {C_{\rm total}}^{0.33\pm0.001}. \tag{12}$$

This correlation is compatible with the result of solar flares (Veronig et al. 2002). Note that the fitting errors are very tiny. Therefore, the 95% confidence regions of fitting uncertainties and the fitting line are overlapped in Figure 2. The correlation coefficient is $r = 0.72$, which indicates that the dependency between the fitting line and data is moderate. The fact that the t-test and F-test also prove this dependency is obvious, where $t_{\rm value} \approx 350.82$ and $F_{\rm value} \approx 123076.52$ are much larger than $t_{2.5\%,114728-2} = 1.96$ and $F_{5\%,1,114728-2} = 3.84$.

We use the properties of superflares from Maehara et al. (2015). In contrast to their work, we obtain an identical correlation in Figure 3. Note that unlike what we get above for other data sets, the duration here is in unit of minutes. This is completely unrelated to the slope of linear regression. Linear fitting gives

$$T_{\rm superflares} \propto {E_{\rm superflares}}^{0.39\pm0.025}. \tag{13}$$

Here, the correlation coefficient is $r = 0.75$. $t_{\rm value} \approx 15.48$, and $F_{\rm value} \approx 239.52$, which is much larger than $t_{2.5\%,187-2} = 1.97$, and $F_{5\%,1,187-2} = 3.89$ respectively. So this linear correlation is strongly subsistent.

4. Correlation between Duration and Energy

In the above section, we find that the slopes of the correlations for GRBs, solar flares, and superflares are similar, which indicates that the physical mechanism for these phenomena is similar. We try to explain the slope of GRBs using magnetic reconnection theory.

We make the first assumption that GRBs release magnetic energy stored in central engine. This assumption is similar to solar flares, which releases magnetic energy stored near Sun spots. The relationship between releasing energy and magnetic energy can be written as

$$E_{\rm GRB} \sim f E_{\rm mag} \propto f B^2 L^3 \sim f B^2 V_{\rm mag}, \quad (14)$$

where f represents the fraction of energy released by magnetic dissipation. L corresponds to the typical length of magnetic reconnection scale, and L^3 represents volume $V_{\rm mag}$, where magnetic energy is stored.

Moreover, with a view of that the flare energy is mainly released through magnetic reconnection, the duration of energy release can be comparable with magnetic reconnection time. This relation can be expressed as

$$T_{\rm duration} \sim \tau_{\rm rec} \sim \frac{\tau_{\rm A}}{M_{\rm A}} \sim \frac{L}{v_{\rm A} M_{\rm A}}, \quad (15)$$

where $\tau_{\rm A} = L/v_{\rm A}$ represents the time of plasma traveling at Alfvén speed. The Alfvén-Mach number $M_{\rm A}$ stands for the reconnection rate, which can be treated as a constant. For GRBs, the Alfvén speed may be close to the speed of light, namely, $v_{\rm A} \sim c$ (Jackson 1975; Lazarian & Vishniac 1999). Naturally, the relation between the duration and releasing energy for one GRB can be expressed as

$$T_{\rm duration} \propto E^{\frac{1}{3}}. \quad (16)$$

The correlation is comparable to what we have obtained in Section 3.

Magnetic reconnection driving solar flares is widely accepted from theorems and observations (Priest 1982; Tsuneta et al. 1992, etc.). We find the correlation of GRBs to be $T_{\rm GRB,duration} \propto {E_{\rm GRB,iso}}^{0.34\pm0.032}$, and the exponent 0.34 ± 0.032 is also compatible with the exponent $1/3$ in Equation (16). Our results suggest that magnetic reconnection may also dominate the energy release of GRBs during prompt emission. To be specific, our findings may support some works that set magnetic reconnection as the mechanism powering GRB emission (Metzger et al. 2011; Zhang & Yan 2011; Zhang & Zhang 2014; Beniamini et al. 2018, etc.). Interestingly, theory (Dai et al. 2006) and observations (Wang & Dai 2013) also support the fact that the magnetic reconnection also account for the X-ray flares of GRBs.

5. Conclusions and Discussion

In this Letter, we find the power-law correlation between isotropic energy and duration of GRBs for the first time. Linear fitting has been performed on these two properties of 386 GRBs, which are observed by *Swift*. We also collect 114,728 solar flares from *RHESSI*, and find that the power-law correlation between the total counts and duration of flares is comparable with the correlation of GRBs. In order to make comparison, we also apply this relation to superflares of solar-type stars from *Kepler*.

Linear regression in log–log fields of GRBs is showed in Figure 1. We find the correlation of GRBs as $T_{\rm duration} \propto {E_{\rm iso}}^{0.34\pm0.032}$, which resembles our findings of stellar superflares as $T_{\rm superflares} \propto {E_{\rm superflares}}^{0.39\pm0.025}$, and solar flares as $T_{\rm solar,duration} \propto {C_{\rm total}}^{0.33\pm0.001}$. The t-test and F-test show that the tendency of this correlation is genuinely credible, even for different data sets. From another aspect, our results approximate the theoretical correlation $T_{\rm duration} \propto E^{\frac{1}{3}}$, which is derived from magnetic reconnection theorems. This comparability firmly supports the theory that magnetic reconnection may dominate the energetic releasing process of GRBs.

We thank the referee for detailed and very constructive suggestions that allowed us to improve our manuscript. We would like to thank H. Yu, G.Q. Zhang, J.S. Wang, and H.C. Chen for suggestions. This Letter is supported by the National Natural Science Foundation of China (grant U1831207).

ORCID iDs

F. Y. Wang https://orcid.org/0000-0003-4157-7714

References

Amati, L., Frontera, F., Tavani, M., et al. 2002, A&A, 390, 81
Beloborodov, A. M., & Mészáros, P. 2017, SSRv, 207, 87
Beniamini, P., Barniol Duran, R., & Giannios, D. 2018, MNRAS, 476, 1785
Carrington, R. C. 1859, MNRAS, 20, 13
Christe, S., Hannah, I. G., Krucker, S., McTiernan, J., & Lin, R. P. 2008, ApJ, 677, 1385
Dado, S., & Dar, A. 2017, arXiv:1712.09319
D'Agostini, G. 2005, arXiv:physics/0511182
Dai, Z., Daigne, F., & Mészáros, P. 2017, SSRv, 212, 409
Dai, Z. G., Wang, X. Y., Wu, X. F., & Zhang, B. 2006, Sci, 311, 1127
Daigne, F., Bošnjak, Ž., & Dubus, G. 2011, A&A, 526, A110
Dainotti, M. G., & Amati, L. 2018, PASP, 130, 51001
Dainotti, M. G., & Del Vecchio, R. 2017, NewAR, 77, 23
Dainotti, M. G., Del Vecchio, R., Shigehiro, N., et al. 2015, ApJ, 800, 31
Dainotti, M. G., Del Vecchio, R., & Tarnopolski, M. 2018, AdAst, 2018, 4969503
Dainotti, M. G., Hernandez, X., Postnikov, S., et al. 2017a, ApJ, 848, 88
Dainotti, M. G., Nagataki, S., Maeda, K., et al. 2017b, A&A, 600, A98
Dainotti, M. G., Petrosian, V., Singal, J., et al. 2013, ApJ, 774, 157
Dainotti, M. G., Postnikov, S., Hernandez, X., et al. 2016, ApJL, 825, L20
Efron, B., & Petrosian, V. 1992, ApJ, 399, 345
Hou, S.-J., Liu, T., Lin, D.-B., Wu, X.-F., & Lu, J.-F. 2013, Feeding Compact Objects: Accretion on All Scales, 290, 223
Jackson, J. D. 1975, Classical Electrodynamics (2nd ed.; New York: Wiley)
Kocevski, D., & Petrosian, V. 2013, ApJ, 765, 116
Kumar, P., & Zhang, B. 2015, PhR, 561, 1
Lazarian, A., & Vishniac, E. T. 1999, ApJ, 517, 700
Levan, A. J., Tanvir, N. R., Starling, R. L. C., et al. 2014, ApJ, 781, 13
Liang, E., & Zhang, B. 2005, ApJ, 633, 611
Littlejohns, O. M., & Butler, N. R. 2014, MNRAS, 444, 3948
Lloyd, N. M., & Petrosian, V. 1999, ApJ, 511, 550
Lloyd-Ronning, N. M., Gompertz, B., Pe'er, A., et al. 2018, arXiv:1809.04190
Lyutikov, M. 2006, NJPh, 8, 119
Lyutikov, M., & Blandford, R. 2003, arXiv:astro-ph/0312347
Maehara, H., Shibayama, T., Notsu, S., et al. 2012, Natur, 485, 478
Maehara, H., Shibayama, T., Notsu, Y., et al. 2015, EP&S, 67, 59
Metzger, B. D., Giannios, D., Thompson, T. A., Bucciantini, N., & Quataert, E. 2011, MNRAS, 413, 2031
MichałowskI, M. J., Xu, D., Stevens, J., et al. 2018, A&A, 616, A169
Montgomery, D. C., Peck, E. A., & Vining, G. G. 2012, Introduction to Linear Regression Analysis (5th ed.; New York: Wiley)
Nagataki, S. 2018, RPPh, 81, 26901
Norris, J. P., Marani, G. F., & Bonnell, J. T. 2000, ApJ, 534, 248
Planck Collaboration, Ade, P. A. R., Aghanim, N., et al. 2016, A&A, 594, A13
Priest, E. R. 1982, (Dordrecht, Holland; Boston: D. Reidel Pub. Co.; Hingham)
Rees, M. J., & Meszaros, P. 1994, ApJL, 430, L93
Rees, M. J., & Mészáros, P. 2005, ApJ, 628, 847
Shibayama, T., Maehara, H., Notsu, S., et al. 2013, ApJS, 209, 5
Spruit, H. C., Daigne, F., & Drenkhahn, G. 2001, A&A, 369, 694

Stanway, E. R., Levan, A. J., Tanvir, N., et al. 2015, MNRAS, 446, 3911
Tsuneta, S., Hara, H., Shimizu, T., et al. 1992, PASJ, 44, L63
Veronig, A., Temmer, M., Hanslmeier, A., Otruba, W., & Messerotti, M. 2002, A&A, 382, 1070
Wang, F. Y., & Dai, Z. G. 2013, NatPh, 9, 465
Wang, F. Y., Dai, Z. G., & Liang, E. W. 2015, NewAR, 67, 1
Wang, J. S., Wang, F. Y., Cheng, K. S., & Dai, Z. G. 2016, A&A, 585, A68
Willingale, R., & Mészáros, P. 2017, SSRv, 207, 63
Yu, H., Wang, F. Y., Dai, Z. G., & Cheng, K. S. 2016, ApJS, 218, 13
Zhang, B., Lü, H.-J., & Liang, E.-W. 2016, SSRv, 202, 3
Zhang, B., & Yan, H. 2011, ApJ, 726, 90
Zhang, B., & Zhang, B. 2014, ApJ, 782, 92
Zhang, F.-W., Fan, Y.-Z., Shao, L., et al. 2013, ApJL, 778, L11
Zhang, G. Q., & Wang, F. Y. 2018, ApJ, 852, 1